

Crystal growth of selected II–VI semiconducting alloys by directional solidification

Part I *Ground-based experiments*

CHING-HUA SU, YI-GAO SHA*, S. L. LEHOCZKY, F. R. SZOFRAN, D. C. GILLIES and S. D. COBB

Space Sciences Laboratory, NASA/Marshall Space Flight Center, and Universities Space Research Association, Huntsville, Alabama 35812, USA

R. N. SCRIPA

University of Alabama at Birmingham, Birmingham, Alabama 35294, USA

A series of $\text{Hg}_{0.84}\text{Zn}_{0.16}\text{Te}$ crystal ingots have been grown from pseudobinary melts by the Bridgman–Stockbarger type directional solidification using a Marshall Space Flight Center/Space Science Laboratory heat-pipe furnace and the ground control experiment laboratory furnace of the crystal growth furnace which was flown on the first United States Microgravity Mission. A number of translation rates and a series of hot- and cold-zone temperatures were employed to assess the influence of growth parameters on the crystal properties for the purpose of optimizing the in-flight growth conditions.

1. Introduction

The growth of homogeneous crystals of mercury-based II–VI alloys, such as mercury zinc telluride ($\text{Hg}_{1-x}\text{Zn}_x\text{Te}$, $0 \leq x \leq 1$), from the melt is a particularly challenging task because their liquidus and solidus temperatures are widely separated. Consequently, their interface segregation coefficient is large. Generally, the density of the mercury compound is larger than that of the other II–VI alloying compound, e.g. ZnTe. This, when combined with the large change in the thermophysical properties upon phase change, makes the achievement and control of the desired solidification interface shape an extremely difficult task in a gravitational environment.

On Earth, the mercury-rich component rejected during solidification is denser than the original melt and the vertical Bridgman–Stockbarger melt-growth process would appear to be both gravitationally and thermally stable against convection. However, this is not generally the case. Owing to the peculiar relationships between the thermal conductivities of the melt, solid, and ampoule, it is not practical completely to avoid radial temperature gradients in the growth region for alloys of this type [1–4]. Because of the high mercury partial vapour pressures involved at the processing temperatures [5–8], the confinement of the alloys requires the use of very thick fused silica ampoules which have thermal conductivities compared to those of the alloys. This, when combined with the large (a factor of 4–10) decrease in the thermal conductivities of mercury-based alloys upon freezing [9–11], leads to isothermal surfaces near the melt/solid interface that are bowed into the solid. Although the interface under this condition is neither an isother-

mal nor an isocompositional surface, it is bowed in the same direction as the adjacent isotherm. A method that relies on a careful control of radiation heat transfer near the growth interface can minimize this effect [1, 4, 12]; nonetheless, because the interface temperature undergoes large changes during growth, the complete elimination of radial temperature gradients in the vicinity of the interface is nearly impossible. Thus, in spite of the stabilizing influence of solutal density gradients, intense thermally driven gravity-induced fluid flows will always occur near the interface [13–16]. Recent theoretical calculations [17] suggest that such flows should have only a small effect on the solidified alloy composition. On the other hand, alteration of the flow field by growing in a magnetic field yielded significant changes in the axial and radial compositional distribution in HgCdTe and HgZnTe alloys for the growth rates and temperature distributions employed [18]. One of the aims of this and other flight experiments [19] was to evaluate the relative importance of various gravity and non-gravity related effects.

2. Ground-based investigation

A series of $\text{Hg}_{0.84}\text{Zn}_{0.16}\text{Te}$ crystal ingots (Table I) have been grown from pseudobinary melts by the Bridgman–Stockbarger type directional solidification using a Marshall Space Flight Center/Space Science Laboratory (SSL) heat-pipe furnace [20] and the Crystal growth furnace (CGF) (Fig. 1) ground control experiment laboratory (GCEL) furnace. A number of translation rates and a series of hot- and cold-zone temperatures were employed to assess the influence of growth parameters on crystal properties.

TABLE I Ground-based $\text{Hg}_{0.84}\text{Zn}_{0.16}\text{Te}$ Alloy Crystals Grown by the Bridgman Stockbarger type directional solidification

Sample	Processed furnace	Growth furnace	Hot-zone temp. (°C)	Cold-zone temp. (°C)	Growth rate (mm d^{-1})	Length growth (mm)
B16-L	SSL	—	790	530	3.8	101.3
B18-K ^a	SSL	SSL	790	550	3.8	29.6
B16-1 ^b	SSL	GCEL(1)	800	375	3.5	10.8
		GCEL(2)	800	375	3.5	10.4
B16-2 ^b	SSL	GCEL(1)	780	350	3.5	8.9
		GCEL(2)	780	350	3.5	11.6
B16-4 ^b	SSL	GCEL(1)	800	555	3.5	21.7
		GCEL(2)	800	555	3.5	7.1
B16-8	GCEL	GCEL	800	350	3.5	17.7
B16-33	SSL	GCEL	800	350	3.5	17.9

^a $\text{Hg}_{0.82}\text{Zn}_{0.18}\text{Te}$ sample.

^b For samples B16-1, 2 and 4 the samples were preprocessed in SSL furnace and back-melted, regrown and quenched in GCEL (GCEL(1)) and then were back-melted and grown again in GCEL (GCEL(2)).

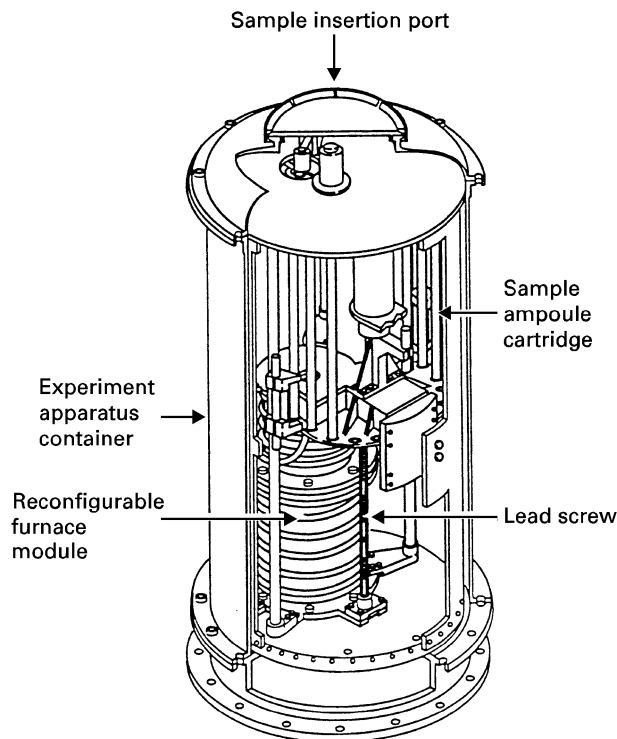


Figure 1 Schematic illustration of the crystal growth furnace.

The ingots were sectioned longitudinally and transversely, polished, and etched appropriately to reveal macroscopic and microscopic defects, including cracks, grain boundaries, voids, second-phase inclusions, and dislocations.

Precision mass density, wavelength-dispersive (WDS) and energy-dispersive X-ray spectroscopy (EDS) analyses were used to generate detailed compositional maps of the ingots. The fitting of the measured axial compositional profiles to a one-dimensional diffusion model which includes changes in the interface temperature and segregation coefficient during the transient phase of solidification [21–24] was used to obtain an estimate for the effective HgTe-ZnTe liquid diffusion coefficient, D , and the fit for an $x = 0.18$ alloy is shown in Fig. 2. A best estimate of $D = 8.0 \times 10^{-6} \text{ cm}^2 \text{ s}^{-1}$ and the pseudobinary phase diagram were used to obtain

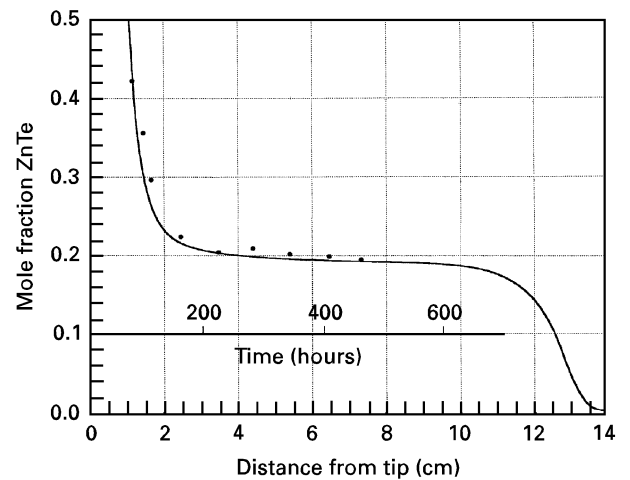


Figure 2 Axial variation in an $\text{Hg}_{0.82}\text{Zn}_{0.18}\text{Te}$ alloy crystal sample B18-K showing measured and calculated results. Effective diffusion coefficient = 8.0×10^{-6} , translation rate = 0.1584 mm h^{-1} , $x = 0.18$, temperature gradient = $65^\circ \text{C cm}^{-1}$, supercooled length = 0.9 cm , total sample length = 14.0 cm .

$G/R = 9.0 \times 10^6 \text{ }^\circ \text{C s cm}^{-2}$ (G is the temperature gradient in the melt ahead of the interface, and R is the solidification rate) as the criterion for the prevention of interface breakdown resulted from constitutional supercooling. For optimum CGF operation conditions, G was estimated to be about $40^\circ \text{C cm}^{-1}$, which allowed a maximum growth rate of about 3.8 mm d^{-1} . The time scale in Fig. 2 illustrates the time-consuming nature of growing a crystal of significant length under steady-state and constant x conditions, and therefore the impossibility of meeting one of the major goals of the flight experiment, growth of homogeneous crystal, within the 150 h mission elapsed time allocated for the experiment. We decided, therefore, to grow the first part, the initial transient segment in Fig. 2, of the crystal on the ground, and then rapidly freeze (quench) the remaining liquid to preserve the melt composition distribution needed for the continuation of steady-state growth following back-melting on orbit. A series of growth runs was performed to establish the required protocols. Four precisely located thermocouples were used to establish the proper back-melting position. The quench was initiated when the

appropriate thermocouple read the solidus temperature of the $x = 0.16$ alloy, i.e. 695°C .

Fig. 3 depicts the grain structure following a typical back-melting/regrowth sequence. As can be inferred

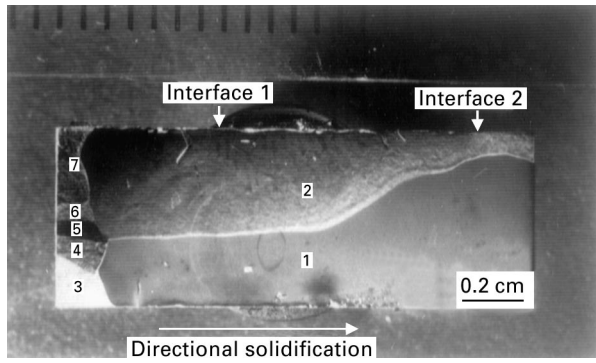


Figure 3 Grain structure near the quenched, back-melted and regrowth interface.

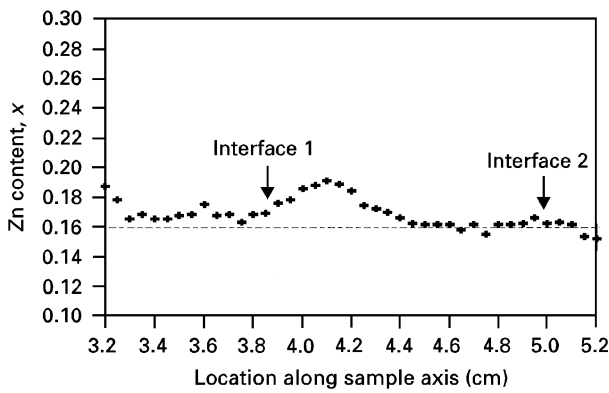


Figure 4 Axial compositional distribution following back-melt/regrowth sequence in $\text{Hg}_{1-x}\text{Zn}_x\text{Te}$, sample B16-1A-B.

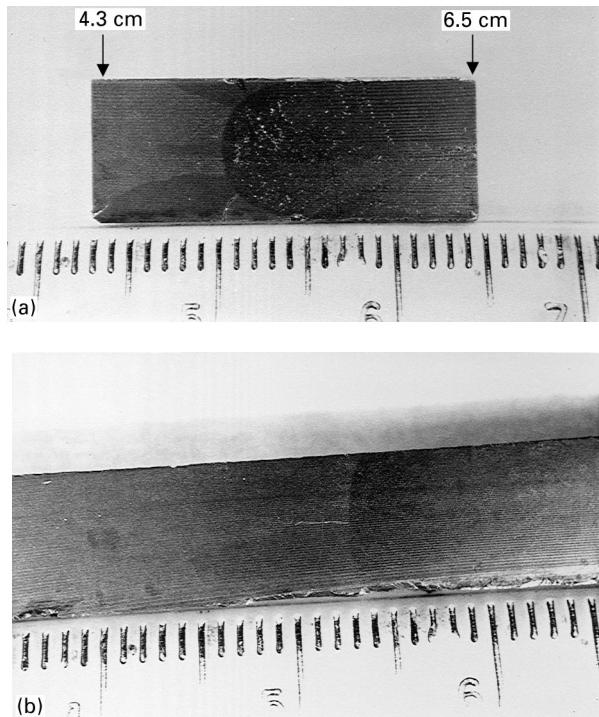


Figure 5 Interface shapes for (a) a hot-zone temperature of 800°C and a cold-zone temperature of 555°C , and (b) a hot-zone temperature of 780°C and a cold zone temperature of 350°C .

from the figure, grain growth usually proceeded as would have been expected had there been no growth interruption. Fig. 4 shows the behaviour of the axial composition distribution prior to and after regrowth for one of the ingots. The data indicate that a nearly steady-state growth resumed following back-melting without any significant composition transients.

Fig. 5 shows the interface region for two different temperature settings. As can be seen the melt/solid interface shapes are highly dependent on the exact temperature settings used. A hot zone temperature of 800°C and a cold zone temperature of 350°C were selected as optimum for the flight experiment. The radial compositional variations for the two cores are illustrated in Figs 6 and 7.

3. Summary of ground-based results

A best estimate for the effective HgTe-ZnTe liquid diffusion coefficient, D , was obtained by fitting the measured axial compositional profile to a one-dimensional diffusion mode. A maximum growth rate of 3.8 mm d^{-1} was then estimated from D , the thermal

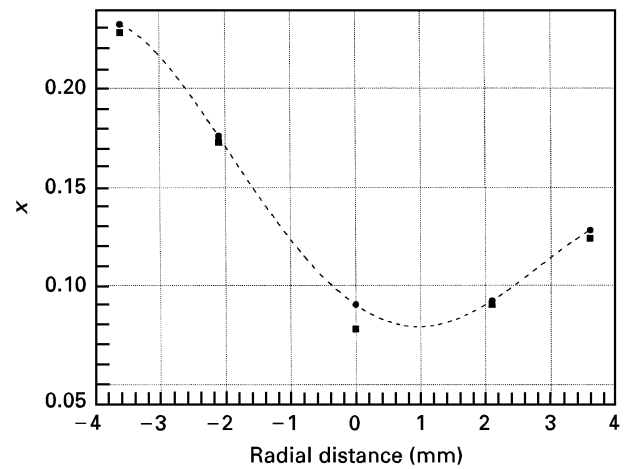


Figure 6 Radial compositional variation for ingot shown in Fig. 5a: (—●—) 1 mm from the interface, (■) 2 mm from the interface.

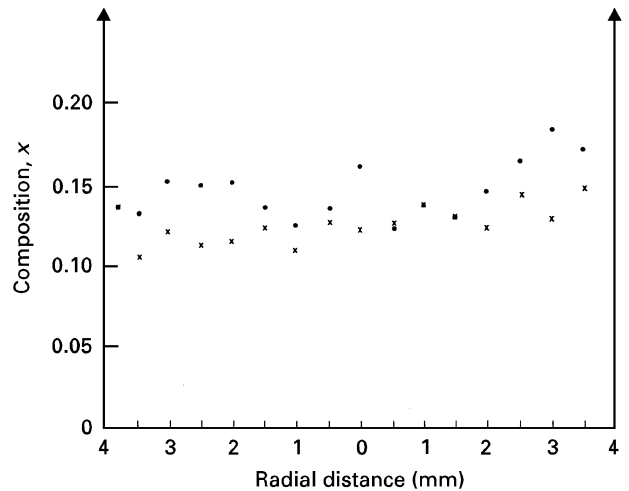


Figure 7 Radial compositional variation for ingot (sample B16-2) shown in Fig. 5b. The data were measured along (●) 3.26 and (×) 4.26 cm from the first freeze (the interface is at about 5.3 cm from the first freeze).

gradient in the melt and the HgTe–ZnTe phase diagram. With the 150 h orbit time allocated for the experiment, the amount of crystal which can be grown was limited to 2 cm. Hence, a back-melting/regrowth sequence was designed for the flight experiment and several ground-based growths demonstrated that partially grown then quenched ingots can be back-melted and regrown without significant interruption in the alloy composition and crystalline structure.

Acknowledgement

The work was supported by the Microgravity Science and Applications Division of NASA.

References

1. F. R. SZOFRAN and S. L. LEHOCZKY, *J. Crystal Growth* **70** (1984) 349.
2. R. J. NAUMANN and S. L. LEHOCZKY, *ibid.* **61** (1983) 707.
3. J. JASINSKI, W. M. ROHSENOW and A. F. WITT, *ibid.* **61** (1983) 339.
4. Y. M. DAKHOUL, R. FARMER, S. L. LEHOCZKY and F. R. SZOFRAN, *ibid.* **86** (1988) 49.
5. J. STEININGER, A. J. STRAUSS and R. F. BREBRICK, *J. Electrochem. Soc.* **117** (1970) 1305.
6. J. STEININGER, *J. Electron. Mater.* **5** (1976) 299.
7. J. D. KELLY, B. G. MARTIN, F. R. SZOFRAN and S. L. LEHOCZKY, *J. Electrochem. Soc.* **129** (1982) 2360.
8. T. C. YU and R. F. BREBRICK, *J. Phase Equilibria* **13** (1992) 476.
9. L. R. HOLLAND and R. E. TAYLOR, *J. Vac. Sci. Technol.* **A1** (1983) 1615.
10. C.-H. SU, *J. Crystal Growth* **78** (1986) 51.
11. F. R. SZOFRAN and S. L. LEHOCZKY, *Bull APS* **28** (1983) 1313.
12. S. D. COBB, R. N. ANDREWS, F. R. SZOFRAN and S. L. LEHOCZKY, *J. Crystal Growth* **110** (1991) 415.
13. S. L. LEHOCZKY and F. R. SZOFRAN, NASA Technical Paper 2787 (December 1987).
14. S. L. LEHOCZKY and F. R. SZOFRAN, in "The Nation's Future Materials Needs", International SAMPE Technical Conference Series, edited by T. Lynch, J. Persh, T. Wolf and N. Rupert (SAMPE: Technical Conference, Arlington, VA, 1987) pp. 13–15.
15. S. D. COBB, F. R. SZOFRAN and S. L. LEHOCZKY, in "AACG/West 10th Conference on Crystal Growth", Fallen Leaf Lake, CA (1988) p. 9.
16. D. H. KIM and R. A. BROWN, Massachusetts Institute of Technology, private communication (1990).
17. *Idem*, *J. Crystal Growth* **114** (1991) 411.
18. C.-H. SU, S. L. LEHOCZKY and F. R. SZOFRAN, *ibid.* **109** (1991) 392.
19. S. L. LEHOCZKY, F. R. SZOFRAN and D. C. GILLIES, NASA Technical Memorandum 4737 (1996) "Second United States Microgravity Payload: One year Report", edited by P. A. Curreri and D. E. Mc Cauley (NASA, 1996) pp. 4–91.
20. S. L. LEHOCZKY, F. R. SZOFRAN and B. G. MARTIN, NASA CR-161598 (1980).
21. J. C. CLAYTON, NASA CR-162049 (1982).
22. J. C. CLAYTON, M. C. DAVIDSON, D. C. GILLIES and S. L. LEHOCZKY, *J. Crystal Growth* **60** (1982) 374.
23. R. N. ANDREWS, F. R. SZOFRAN and S. L. LEHOCZKY, *ibid.* **92** (1988) 445.
24. F. R. SZOFRAN, D. CHANDRA, J.-C. WANG, E. K. COTHRAN and S. L. LEHOCZKY, *ibid.* **70** (1984) 343.

*Received 20 November 1995
and accepted 10 February 1996*